Prediction of rapid amyloid and phosphorylatedTau accumulation in cognitively healthy individuals

Received: 15 November 2019 | Revised: 31 January 2020 | Accepted: 3 February 2020 | Published online: 23 March 2020

DOI: 10.1002/dad2.12019

Alzheimer's & Dementia
Diagnosis, Assessment & Disease Monitoring

CEREBROSPINAL FLUID BIOMARKERS

Prediction of rapid amyloid and phosphorylated-Tau accumulation in cognitively healthy individuals

Ivan Koychev[1] | Nemanja Vaci[1] | Murat Bilgel[2] | Yang An[2] | Graciela Terrera Muniz[3] | Dean F. Wong[4] | John Gallacher[1] | Abhay Mogekhar[5] | Marilyn Albert[5] | Susan M. Resnick[2]

[1]Department of Psychiatry, University of Oxford, Oxford, UK

[2]Laboratory of Behavioral Neuroscience, National Institute on Aging, National Institutes of Health, Baltimore, Maryland

[3]Centre for Dementia Prevention, The University of Edinburgh, Edinburgh, UK

[4]Department of Radiology, Johns Hopkins School of Medicine, Baltimore, Maryland

[5]Department of Neurology, Johns Hopkins School of Medicine, Baltimore, Maryland

Correspondence
Dr Ivan Koychev, Department of Psychiatry, Warneford Hospital, Warneford Lane, Oxford, OX3 7JX, UK.
Email: ivan.koychev@psych.ox.ac.uk

Abstract

Objective: To test the hypothesis that among cognitively healthy individuals, distinct groups exist in terms of amyloid and phosphorylated-tau accumulation rates; that if rapid accumulator groups exist, their membership can be predicted by Alzheimer's disease (AD) risk factors, and that time points of significant increase in AD protein accumulation will be evident.

Methods: The analysis reports data from 263 individuals from the BIOCARD and 184 individuals from the Baltimore Longitudinal Study of Aging with repeated cerebrospinal fluid (CSF) and positron emission tomography (PET) sampling, respectively. We used latent class mixed-effect models to identify distinct classes of amyloid (CSF and PET) and p-Tau (CSF) accumulation rates and generalized additive modeling to investigate non-linear changes to AD biomarkers.

Results: For both amyloid and p-Tau latent class models we confirmed the existence of two separate classes: accumulators and non-accumulators. The accumulator and non-accumulator groups differed significantly in terms of baseline AD protein levels and slope of change. *APOE* ε4 carrier status and episodic memory predicted amyloid class membership. Non-linear models revealed time points of significant increase in the rate of amyloid and p-Tau accumulation whereby *APOE* ε4 carrier status associated with earlier age at onset of rapid accumulation.

Conclusions: The current analysis demonstrates the existence of distinct classes of amyloid and p-Tau accumulators. Predictors of class membership were identified but the overall accuracy of the models was modest, highlighting the need for additional biomarkers that are sensitive to early disease phenotypes.

KEYWORDS

amyloid, CSF, emerging Alzheimer's disease pathology, positron emission tomography, phosphorylated tau

1 | BACKGROUND

Evidence of abnormal amyloid burden ("amyloid positivity") is now a standard inclusion criterion for clinical trials of disease modification agents in pre-dementia Alzheimer's disease (AD).[1,2] However, recent evidence has challenged the notion that widespread amyloid pathology is required before downstream neurodegenerative effects are evident and argue for the existence of clinically relevant "emerging amyloid

pathology."[3] Specifically, cognitively healthy individuals classed as "amyloid negative" but with evidence for steep slope of amyloid accumulation have increased frontoparietal atrophy rates,[4] memory decline,[5] and tau accumulation.[6] In addition, evidence exists for tau emerging independently and earlier than amyloid[7] and thus identifying individuals on an aggressive tau accumulation trajectory in conjunction with amyloid or on its own[8] is of interest. Furthermore, the rate of increase in AD biomarkers does not appear to follow a linear course but rather features points of acute acceleration.[9,10] Taken together these data argue that an intervention's impact is likely to be greatest if delivered (1) to individuals on aggressive trajectory of AD protein accumulation and (2) in temporal proximity to time points of rapid AD protein burden acceleration.

In this analysis we sought to identify whether subgroups of rapid AD protein accumulators exist among initially cognitively healthy individuals in two large longitudinal cohorts sampling cerebrospinal fluid (CSF) and positron emission tomography (PET), respectively. We hypothesized that if rapid accumulator groups exist, their membership can be predicted by AD risk factors and that time points of significant increase in AD protein accumulation will be evident.

RESEARCH IN CONTEXT

1. Systematic review: The authors reviewed the literature using traditional (eg, PubMed) sources. The concept of "emerging amyloid pathology" is gathering momentum, and recent evidence of pathophysiological relevance of rapid Alzheimer's disease (AD) protein accumulation in the absence of biomarker "positivity" is appropriately cited.
2. Interpretation: Our findings demonstrate that repeated AD protein sampling through cerebrospinal fluid (CSF) and positron emission tomography (PET) in initially cognitively healthy individuals allows the identification of distinct groups of accumulators and non-accumulators in respect to both amyloid and p-Tau. In addition, critical time points of significant escalation in accumulation occur and these are APOE4 dependent.
3. Future directions: Development of novel treatments targeting AD pathology can be boosted by targeting pre-symptomatic individuals on an aggressive accumulation trajectory. Prediction of accumulator group membership was modest based on established AD risk factors in this study, which emphasizes the need to develop biomarkers specific to the preclinical stage of the disease.

2 | METHODS

2.1 | Study design and participants

The study reports data from the Biomarkers of Cognitive Decline Among Normal Individuals (BIOCARD) and Baltimore Longitudinal Study of Aging (BLSA) studies. BIOCARD was established in 1995 by the National Institutes of Health (NIH). The goal was to evaluate risk factors for progression to AD among cognitively healthy individuals. The study was stopped in 2005 and re-started at Johns Hopkins University (JHU) in 2009. Between 1995 and 2005, participants were assessed cognitively and clinically annually with CSF, blood sampling, and magnetic resonance imaging (MRI) collection every 2 years. Since 2009, participants have been seen annually for clinical, cognitive assessments and to provide blood samples. In 2015, bi-annual collection of MRI and CSF was re-started. Exclusion criteria were (1) cognitive impairment as determined by cognitive testing; (2) significant medical or neurological conditions (eg, atrial fibrillation, epilepsy, multiple sclerosis); and (3) chronic psychiatric disorders (eg, schizophrenia, drug or alcohol abuse/dependence).

The BLSA sample included participants from its neuroimaging sub-study, which was initiated in 1994 and included annual MRI evaluations.[11] At enrollment, participants were free of central nervous system (CNS) disease (dementia, stroke, bipolar illness, epilepsy), and severe cardiac (myocardial infarction, coronary artery disease requiring angioplasty, or coronary artery bypass surgery), pulmonary, or metastatic disease. Since 2003, participants were assessed every 1 (if older than 80 years), 2 (ages 60–79), or 4 years (younger than 60 years). Beginning in 2005, participants were imaged with ^{11}C-Pittsburgh compound B (PiB) amyloid PET.

2.2 | Participants

We focused on participants who had CSF (BIOCARD) or PET (BLSA) testing. Included participants were aged >40 years and had Mini-Mental State Examination (MMSE) ≥ 25 at first CSF or PET measurement. This resulted in 588 CSF data points for 263 participants (BIOCARD) and 496 PET observations for 184 participants (BLSA); see descriptives in Table 1.

2.3 | Cognitive assessments

We selected two cognitive measures that were shared between the two studies: the long delayed free recall variable of the California Verbal Learning Test (CVLT) and total score of the MMSE.

2.4 | Genetic analysis

APOE ε4 status was determined using standard procedures[12] or TaqMan.[13] We coded participants into two groups: those with and without *APOE* ε4 carriership.

TABLE 1 Demographics, cognitive scores, and number of CSF and MRI individual data points per individual

	BIOCARD		BLSA	
Variables	**Mean (SD)**	**Range**	**Mean (SD)**	**Range**
Age at baseline	58 (8.2)	42–64	79 (8.1)	55–95
Education	17 (2.4)	12–20	17 (2.3)	8–21
MMSE (first observation)	29.5 (0.8)	25–30	28.7 (1.2)	25–30
MMSE (last observation)	29.4 (1.03)	23–30	28.3 (1.5)	22–30
No. of CSF/PET measurements	2.2 (1.3)	1–6	2.6 (1.9)	1–9
MRI measurements	2.0 (1.1)	1–5	2.3 (1.7)	1–9
	Percentage (N = 263)		**Percentage (N = 184)**	
% Female (N)	59% (154)		48% (88)	
% Caucasian N	97% (255)		78% (143)	
% *APOE* ε4 carriers (%)	36% (95)		30% (57)	

APOE, apolipoprotein E gene; CSF, cerebrospinal fluid; MMSE, Mini-Mental State Examination; MRI, magnetic resonance imaging.

2.5 | CSF analysis

CSF was collected after an overnight fast into polypropylene tubes, and Aβ1-42 and p-Tau181 were measured on the Luminex platform using the AlzBio3 kit (4D7A3 and AT270 monoclonal antibodies, respectively). Each subject had all samples (run in triplicate) analyzed on the same plate.[14]

2.6 | MRI

For BIOCARD, baseline MRI scans were acquired at the NIH on a GE 1.5T scanner using a standard multimodal protocol. The baseline MRI measures that were used as part of the biomarker composite score were reconstructed from coronal spoiled gradient echo scans (repetition time [TR] = 24 ms, echo time [TE] = 2 ms, flip angle = 20°, image matrix = 256 × 256 mm, thickness/gap = 2.0/0.0 mm, 124 slices). The mean time between the baseline MRI scan and the baseline cognitive assessment was 8.6 days (standard deviation [SD] = 40.4, range = 0-362). The volume of the hippocampus was obtained with a semi-automated method, based on large deformation diffeomorphic metric mapping techniques, which included adjustment for intracranial volume.[15]

In the case of BLSA data, magnetization-prepared rapid gradient echo (MPRAGE) images were acquired either on a 3 T Philips Achieva scanner (TR = 6.8 ms, TE = 3.2 ms, flip angle = 8°, image matrix = 256 × 256 mm, 170 slices, pixel size = 1 × 1 mm, slice thickness = 1.2 mm) or a 1.5 T Philips Intera scanner (TR = 6.8 ms, TE = 3.3 ms, flip angle = 8°, image matrix = 256 × 256 mm, 124 slices, pixel size = 0.94 × 0.94 mm, slice thickness = 1.5 mm), or spoiled gradient-recalled images were acquired on a 1.5 T GE Signa scanner (TR = 35 ms, TE = 5 ms, flip angle = 45°, image matrix = 256 × 256 mm, 124 slices, pixel size = 0.94 × 0.94 mm, slice thickness = 1.5 mm). Anatomical labels and regional brain volumes were obtained using MUlti-atlas region Segmentation using Ensembles of registration algorithms and parameters[16] with atlases that have been harmonized to account for differences in scanners and acquisition parameters.[17] We corrected for intracranial volume estimated at age 70 using a residual volume approach described earlier.[18] Residual volumes were computed for each region and each scan as the difference, in mm^3, of the measured regional volume from the regional volume that would be expected given the ICV of the individual.

2.7 | PET analysis

Dynamic ^{11}C-PiB PET studies (3D mode on GE Advance scanner) started immediately after intravenous bolus injection of 555 MBq (15 mCi) of ^{11}C-PiB. Dynamic images were reconstructed using filtered back-projection with a ramp filter to yield 33 time frames over 70 minutes (4 × 0.25, 8 × 0.5, 9 × 1, 2 × 3, and 10 × 5 minutes), with a spatial resolution of approximately 4.5 mm full width at half maximum (FWHM)at the center of the field of view (image matrix = 128 × 128, 35 slices, voxel size = 2 × 2 × 4.25 mm).

Each of the 33 timeframes was aligned to the mean of the first 2 minutes to correct for motion using SPM's Realign (https://www.fil.ion.ucl.ac.uk/spm/software/spm12/).[19] The average of the first 20 minutes of PET scans was rigidly registered onto the corresponding inhomogeneity-corrected MPRAGE, and the anatomical label image was transformed from MRI to PET space using FLIRT[20] implemented in FSL (https://fsl.fmrib.ox.ac.uk/fsl, version 5.0).[21] Distribution volume ratio (DVR) images were computed in PET native space using a simplified reference tissue model[22] with cerebellar gray matter as the reference region. Mean cortical amyloid β (Aβ) burden was calculated as the average of the DVR values in cingulate, frontal, parietal (including precuneus), lateral temporal, and lateral occipital cortical regions, excluding the sensorimotor strip.

2.8 | Statistical analysis

We used latent class mixed-effect models[23] to identify distinct classes of individuals with similar longitudinal patterns of AD biomarker

change (CSF Abeta-42 and p-Tau in BIOCARD; mean amyloid cortical DVR in BLSA). The intercept of the model was centered on 40 years of age for BIOCARD and 55 years for BLSA, adjusting it for the earliest age at which AD proteins are sampled. The latent class mixed-effect model uses a random-effect structure when estimating heterogeneity between individuals' growth curves, allowing estimates of potential different classes of accumulators and probabilities of class membership. We calculated the differences between the groups on the variables of interest and combined this analysis with logistic regression to investigate prediction of class membership. Where repeated measures were available for the predictors (MMSE, episodic memory, hippocampal volume) we used their average values over the study duration. The class interpretation, together with the Akaike, Bayesian, and sample-size adjusted Bayesian information criteria (AIC, BIC, and SABIC, respectively), was used to compare models with different levels of complexity.

To investigate the nonlinearity of change of AD-related CSF and PET biomarkers and impact of hypothesized predictors we used generalized additive mixed-effect models (GAMs[24]). Mixed-effect models allow us to account for time-related repeated measures per participant by including a random structure, that is, participants' unique effects in regression. In other words, our models take into account variability in the baseline of amyloid and p-tau protein levels, as well as, speed of accumulation when fitting the general age-related changes. We estimated the age-related function of AD biomarkers and explored the impact of *APOE* ε4 status on these changes. We also investigated periods of statistically significant changes in the slope of the nonlinear function[25] taking into account *APOE* ε4 using finite differences method.[26] The idea behind this method is to replace continuous prediction of the model by the discrete points placed across variable of interest (age—in this study). We then approximate derivatives between each pair of points to obtain changes of dependent variable (ie, CSF amyloid accumulation) across the independent predictor (ie, age). Finally, we take into account uncertainty of prediction (lower and upper 95% confidence interval [CI]) to infer whether this change is statistically significant. All models, R code, as well as, main and supplementary results are reported in online materials https://osf.io/fcuyd/).

To estimate the clinical impact of being classed as an accumulator or non-accumulator we used mixed-effect Cox regression fitted on the longitudinal observations in the BIOCARD data. In these models, we investigated whether the likelihood of being diagnosed with cognitive impairment or dementia changes dependent on membership in amyloid accumulator, p-Tau accumulator, or both or neither groups.

3 | RESULTS

3.1 | Latent class modeling: amyloid

We investigated the existence of distinct groups underlying the pattern of amyloid (CSF and PET amyloid separately) and p-Tau (CSF) accumulation by using latent class mixed-effect modeling. The model included random intercept adjustments for participants, as well as random slopes for influence of age. Results confirmed our hypothesis that two separate groups of participants existed in the case of amyloid for both CSF and PET: non-accumulators and accumulators (Figure 1A and 1B; see Table 2 for demographics and clinical data). With regard to the CSF amyloid levels, the group of non-accumulators was characterized by significantly higher intercept and shallower decline over time (see Table 3). In contrast, the accumulators tended to have lower intercept and steeper accumulation of amyloid over time, that is, reduction in CSF Abeta-42 levels (see Figure 1C). Classification of participants into these two groups resulted in 197 participants assigned to the non-accumulator group with an average probability of 0.81 and 66 participants assigned to the accumulator group with an average probability of 0.89.

An identical pattern occurs in PET amyloid, where the accumulator group was characterized by higher intercept and steeper increase over time relative to the non-accumulator group. The classification of the sample into two groups resulted in 144 people being classified as non-accumulators, with an average probability of 0.99 and 40 people being assigned to the accumulator group with average probability of 0.98. AIC, BIC, and SABIC model comparisons confirmed that a two-group separation is the best fit for the CSF amyloid, PET amyloid, and CSF tau models (see supplementary materials for model comparisons).

3.2 | Predicting amyloid latent class: CSF and PET

Next we tested whether prediction of the latent class of amyloid progression in CSF and PET can be made using logistic regression with the probit link function. In the case of CSF-derived amyloid, results show that *APOE* ε4 carriership increases the probability of belonging to the accumulator group (Table 4). Episodic memory (long delayed recall of the CVLT) was the only other significant predictor whereby lower numbers of recalled words associated with higher likelihood of belonging to the accumulator group. Years of education approached significance, with higher education increasing the probability of belonging in the non-accumulator group. The logistic model reached 0.77 accuracy with 0.08 sensitivity and 0.98 specificity at the 0.5 threshold, whereas the area under the curve was 0.66.

The PET-derived amyloid model replicated the effect of *APOE* ε4, whereby carriers had an increased probability of belonging to the accumulator group. Neither episodic memory, measured as delayed recall, nor years of education was a statistically significant predictor in this model. The logistic model reached 0.81 accuracy, with 0.171 sensitivity and 0.992 specificity at the 0.5 threshold, while the area under the curve was 0.69.

3.3 | Latent class modeling: p-Tau (CSF)

Similar to the amyloid analyses, the latent class mixed-effect regression suggested the existence of two different groups of p-Tau accumulators (Figure 1C; see cross-validation subchapter in supplementary materials). The validity of the latent class modeling was supported by AIC

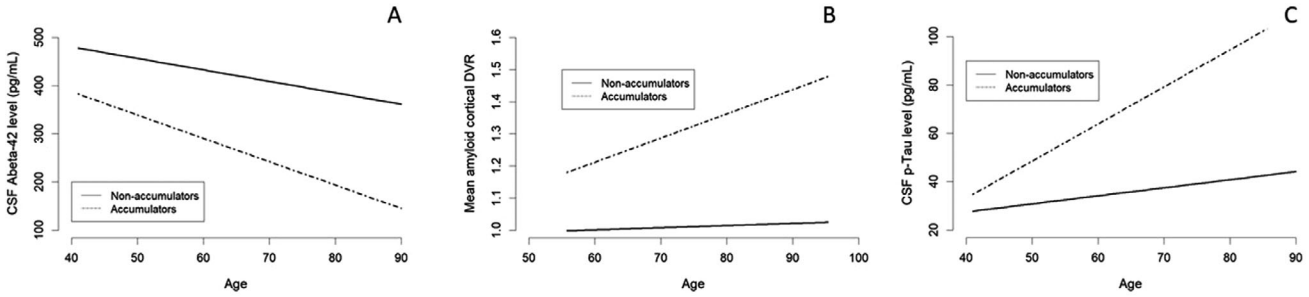

FIGURE 1 Alzheimer's disease (AD) protein intercept and change over time for two distinct accumulation groups in the BIOCARD and BLSA cohorts. Plots represent BIOCARD amyloid cerebrospinal fluid (CSF) concentration (A), positron emission tomography (PET) mean cDVR (B), and BIOCARD tau CSF levels (C). Accumulator classes shown in dotted line; non-accumulators shown in solid line

TABLE 2 Demographics, cognitive scores, and number of CSF and MRI individual data points per individual for the two BLSA latent classes (amyloid accumulators and non-accumulators) and the four latent classes in the BIOCARD study (amyloid accumulators, P-Tau accumulators, amyloid and P-tau accumulators, and non-accumulators)

	BLSA			BIOCARD		
Variables	Amyloid PET accumulators Mean (SD)	Amyloid PET non-accumulators Mean (SD)	Amyloid CSF accumulators Mean (SD)	p-Tau CSF accumulators Mean (SD)	Amyloid and p-Tau CSF accumulators Mean (SD)	CSF Non-accumulators Mean (SD)
Age at baseline	79.2 (7.0)	75.2 (8.3)	58.6 (8.3)	58.1 (6.6)	64.1 (8.2)	58.6 (8.3)
Education	16.7 (2.3)	17.3 (2.2)	16.4 (2.7)	17.7 (1.4)	16.7 (2.6)	17.2 (2.3)
MMSE (first observation)	28.7 (1.0)	28.8 (1.3)	29.4 5 (1.1)	29.7 (0.5)	29.7 (0.5)	29.5 (0.8)
MMSE (last observation)	28.4 (1.4)	28.7 (1.4)	29.4 (1.3)	29.7 (0.5)	28.3 (2.3)	29.5 (0.7)
N of CSF/PET measurements	3.2 (2.2)	2.6 (1.9)	2.0 1 (1.4)	3.6 (1.4)	2.7 (1.2)	2.2 (1.3)
MRI measurements	3.2 (2.2)	2.6 (1.9)	1.9 (1.1)	3.1 (1.0)	2.5 (0.9)	1.9 (1.1)
Average follow-up years	1.55 (0.8)	1.83 (0.9)	1.89 (0.6)	1.88 (0.3)	1.73 (0.5)	2.07 (0.8)
	Percentage (N = 40)	Percentage (N = 144)	Percentage (N = 51)	Percentage (N = 7)	Percentage (N = 15)	Percentage (N = 190)
% Female (N)	35% (14)	51% (74)	49% (25)	71%(5)	60% (9)	60% (115)
% Caucasian (N)	82% (33)	76% (110)	96% (49)	100% (7)	100% (15)	96% (184)
% *APOE* ε4 carriers (N)	52% (21)	25% (36)	50% (26)	57% (4)	46% (7)	30% (58)

APOE, Apolipoprotein E gene; CSF, cerebrospinal fluid; MMSE, Mini-Mental State Examination; MRI, magnetic resonance imaging.

TABLE 3 Summary of the amyloid level intercept and change over time for amyloid accumulators and non-accumulators for CSF (BIOCARD) and PET (BLSA)

	BIOCARD (CSF Amyloid)							
	Accumulators (N = 66)				Non-Accumulators (N = 197)			
	Intercept (SE)	*p*	Age (SE)	*p*	Intercept (SE)	*p*	Age (SE)	*p*
Estimate	387.78 (41)	.0000	−4.847 (1.47)	.001	480.41 (15)	.0000	−2.374 (0.81)	.003
	BLSA (PET Amyloid)							
	Accumulators (N = 40)				Non-Accumulators (N = 144)			
	Intercept (SE)	*p*	Age (SE)	*p*	Intercept (SE)	*p*	Age (SE)	*p*
Estimate	1.17 (0.029)	.0000	0.0075 (0.001)	.000	0.99 (0.01)	.0000	0.0006 (0.0004)	.167

and BIC comparisons. The p-Tau non-accumulators were characterized by a lower baseline level as well as shallower increase over time compared with the group of p-Tau accumulators (see Table 5 and Figure 1C). Classification of participants into these two groups resulted in 241 participants being assigned to the non-accumulator group with average probability of 0.96 and 22 participants to the accumulator group with average probability of 0.85. None of the predictors of p-Tau accumulator class reached statistical significance.

TABLE 4 Summary of predictors of amyloid accumulator class membership for CSF and PET-derived amyloid levels (BIOCARD and BLSA studies respectively)

BIOCARD				
Coefficients	**Estimate**	**Std. error**	**z value**	**Pr (>|z|)**
Intercept	0.220	4.24	0.048	.961
***APOE ε4* carriership**	**0.531**	**0.20**	**2.623**	**.008**
Sex (women)	−0.164	0.20	−0.783	.433
Race (non-white)	−0.413	0.68	−0.601	.547
Hippocampal volume (residuals)	−0.0002	0.00041	−0.488	.625
Years of education	−0.073	0.041	−1.759	.078
MMSE total score	0.049	0.142	0.350	.726
CVLT free recall (long)	**−0.071**	**0.034**	**−2.038**	**.041**
BLSA				
Intercept	−0.85	3.13	−0.272	.785
***APOE ε4* carriership**	**0.714**	**0.24**	**2.964**	**.003**
Sex (women)	−0.36	0.25	−1.274	.202
Race (non-white)	−0.26	0.29	−0.893	.371
Hippocampal volume	−0.19	0.17	−1.088	.276
Years of education	−0.07	0.049	−1.572	.115
MMSE total score	0.04	0.112	0.393	.696
CVLT free recall (long)	−0.001	0.041	−0.024	.980

All predictors are based on averaged measurements per participant. Apolipoprotein E gene (*APOE*), California Verbal Learning Task (CVLT).

TABLE 5 Summary of the CSF p-Tau level intercept and decline over time for accumulators and non-accumulators

	BIOCARD (CSF p-Tau)							
	Accumulators (N = 22)				Non-accumulators (N = 241)			
	Intercept Est(SE)	*p*	Age	*p*	Intercept	*p*	Age	*p*
Estimate	33.21	.0026	1.534	.000	27.45	.0000	0.333	.003

3.4 | Amyloid and p-Tau subclasses: clinical impact

Classifying study participants into amyloid and p-Tau accumulators allowed the generation of a 2 × 2 grouping in BIOCARD with the following groups: non-accumulators for both, amyloid accumulators only, p-Tau accumulators only, and both amyloid and p-Tau accumulators. Breakdown of dementia-related eventual clinical diagnoses at last study visit for the four groups revealed that the group of amyloid and p-Tau accumulator had a 23% prevalence of clinical diagnoses (dementia, MCI, impaired non-MCI), whereas in the amyloid only group it was 11%. None of the participants in the p-Tau accumulator group had a clinical diagnosis, whereas 4% in the non-accumulator group had been diagnosed. Mixed-effect Cox-regression analysis, that included adjustments of the intercept estimates for participants, revealed that only the amyloid accumulator group was predictive of dementia-related diagnosis ($\beta = 1.22$, $\exp(\beta) = 3.39$, SE = 0.63, $z = 1.94$, $p = .05$), when controlling for age and *APOE* ε4 status (see Cox regression in supplementary materials). The lack of statistically significant effect in the p-Tau accumulator group is probably due to the low number of cases.

3.5 | Non-linear model: age and *APOE ε4*

The age-related model revealed a non-linear rate of accumulation for CSF- and PET-derived amyloid (Figure 2) across participants' age. In the case of CSF, the statistically significant decline occurred between the ages of 57 and 77. Stratifying the data set in terms of *APOE* ε4 showed that non-carriers started declining significantly in their CSF amyloid level after the age of 58 (Figure 2, upper left panel), whereas the change started from the age of 53 in carriers and continued until the age of 90 (Figure 2, upper right panel). In the case of PET amyloid, we observed an exponential increase in amyloid burden as individuals aged (see Figure 2). Statistically significant increase started at the age of 68 and continued throughout the lifetime. The function was modulated by *APOE* ε4, whereby carriers started to accumulate amyloid significantly faster at the age of 60 (Figure 2, bottom right panel), whereas non-carriers started increasing at the age of 69 (Figure 2, bottom left panel).

In the case of p-Tau, significant increases were observable between the ages of 55 and 73 (Figure 3). Stratifying by *APOE* ε4 revealed that non-carriers started to show increases in CSF p-Tau approximately when they were 59-years-old (Figure 3, left panel). In contrast,

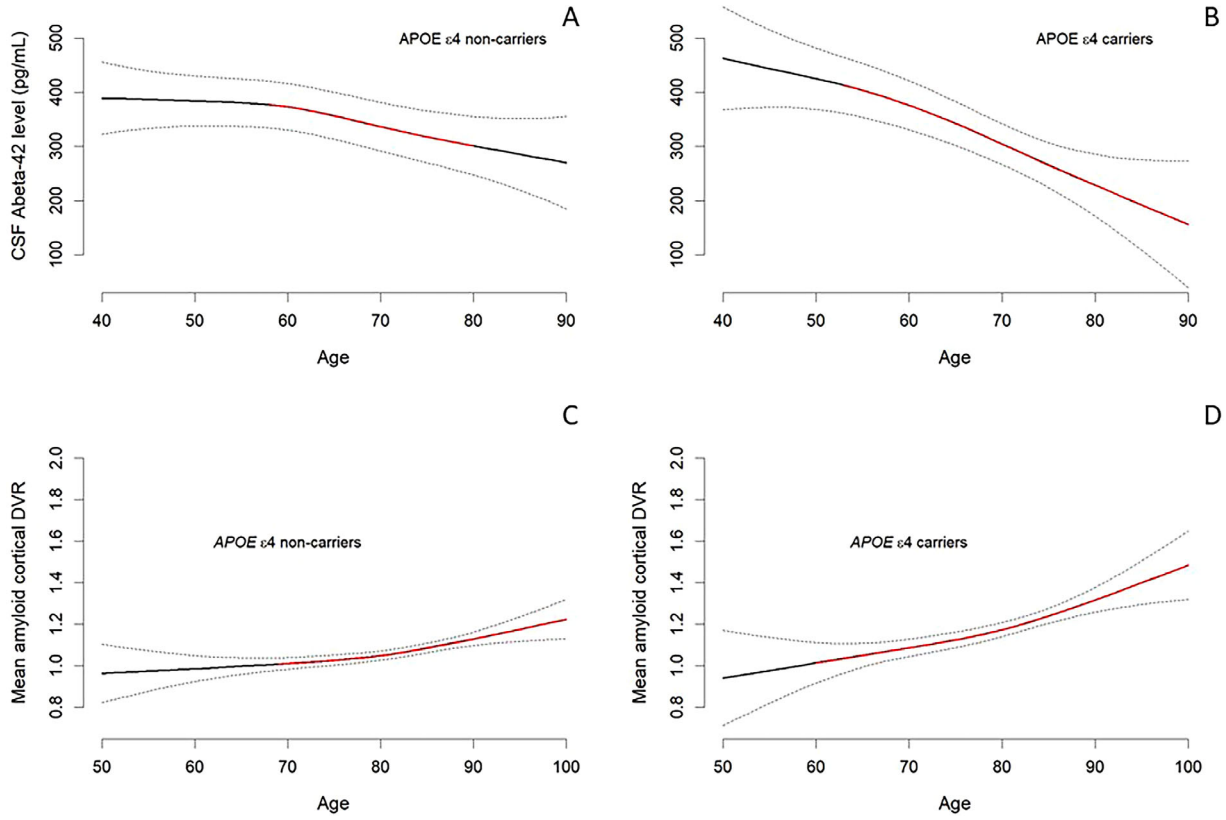

FIGURE 2 Non-linear accumulation of AD biomarkers across participants' age: CSF Abeta-42 (upper panels) and PET amyloid (bottom panels). The red area of the curve indicates statistically significant periods of changes in the age-related function. The age-related changes are modulated by *APOE* ε4 status. (See non-carriers (panels on the left) and carriers (panels on the right) presented separately)

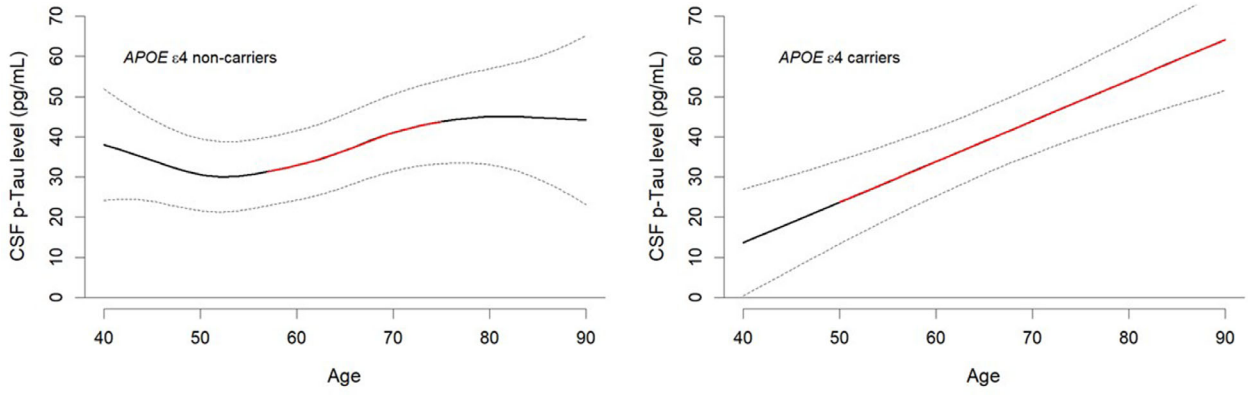

FIGURE 3 Non-linear accumulation of CSF p-Tau across age in BIOCARD. The red area of the curve indicates statistically significant periods of increases in the age-related function. The age-related changes are modulated by *APOE* ε4. Non-carriers (panels on the left) and carriers (panels on the right) presented separately

APOE ε4 carriers started to accumulate p-Tau at the age of 40 (Figure 3, right panel) and the pattern of increase in this group remained linear thereafter.

4 | DISCUSSION

In this study, we sought to establish whether distinct subtypes of AD biomarker progression exist. Analyses for both amyloid and p-Tau yielded two classes for each—faster and slower AD protein accumulators. Although we successfully identified predictors for class membership, the overall accuracy of the models was modest. We also explored the non-linear dynamics of amyloid and p-Tau concentrations' relationship with age. We found that as predicted from previous studies, amyloid concentrations remain largely static until the mid-50s, with evidence for rapid increase of accumulation thereafter. The relationship was similar for p-Tau, and we found that the age of significant change was 57 for amyloid and 55 for p-tau. The non-linear rate of

progression was influenced by *APOE* ε4 status, whereby having at least one allele led to a sharp increase in AD protein burden at a younger age.

The amyloid latent class result represents an extension of prior findings on amyloid accumulators. That higher baseline amyloid burden predicts faster accumulation is known from PET[3,5,27] and CSF studies.[28,29] *APOE* ε4 was a significant predictor of membership to the faster accumulation group. The modulating effect of *APOE* ε4 on rate of amyloid accumulation extends our group's previous analysis on a smaller proportion of the BLSA cohort,[30] which showed that *APOE* ε4 associates with higher likelihood for and earlier onset of cortical amyloid accumulation. It is also consistent with established meta-analytic evidence for earlier and faster amyloid deposition in individuals with this genotype.[31] Studies reporting intra-individual AD biomarker changes as a function of *APOE* ε4 status, however, have been conflicting. For example, although *APOE* ε4 was associated with amyloid accumulation among initially cognitively healthy elderly individuals,[32] reports from the ADNI study did find this using either amyloid PET[5] or CSF.[29] The difference could lie in the longer duration of follow-up and more frequent measurement in the positive studies versus the ADNI analyses.

Episodic memory was a significant predictor in the CSF but not the PET amyloid models. The CSF result follows evidence that amyloid accumulation associates with amnestic but not executive function or processing-speed deficits.[33,34] A potential reason for the lack of effect in the PET analysis is that the BLSA sample was significantly older than BIOCARD (mean ages 76 vs 58). Thus it is possible that the effect of amyloid accumulation on cognition is particularly impactful at younger ages, supporting further the need for interventions to be deployed early in the lifespan.

Distinct classes of p-Tau accumulation were also identified. Faster accumulation associated with higher baseline p-Tau thus replicated the relationship observed for amyloid. The result is consistent with studies showing that baseline p-Tau levels predict progression to impairment in initially cognitively normal individuals.[35] Taken together the amyloid and tau accumulator findings demonstrate the potential for identifying those at risk for faster progression while still in the preclinical stages of the disease.

The non-linear relationships between AD biomarkers and age we describe represent an important extension of the existing literature. A meta-analysis of PET studies has already demonstrated that a significant increase in amyloid deposition begins at the age of 50.[31] However, cross-sectional nature of the observations limit the conclusions that can be drawn about individual trajectories. Here, using a sample consisting of CSF and PET measurements spanning over 20 and 14 years, respectively, we are able to show that even in those with no *APOE* ε4 alleles, a sharp inflection in the accumulation of both amyloid and p-Tau occurs, although at a later point in life relative to those with *APOE* ε4 alleles (on average 8 years later). The design of the current analysis allowed us to compare the time point of amyloid change between PET and CSF, revealing that detectable change occurs 10 years earlier in CSF relative to PET. This result is consistent with established models of sequential biomarker change in AD, which argues that CSF biomarkers are the first to become abnormal.[36] The importance of considering non-linear effects is highlighted by one other study in longitudinal CSF that found both elevations and reductions in amyloid to associate with an increase in p-Tau/tau.[9]

Our CSF finding of amyloid and p-tau beginning their significant change from baseline at approximately the same age (57 for amyloid and 55 for p-tau) is potentially important, as it has relevance to the hypothesis that widespread amyloid burden is required to trigger excessive tau hyperphosphorylation.[36] The extent to which this sequential turn of events can be evidenced in practice, however, has been hampered by the lack of appropriate middle-age sampling as well as within-subject longitudinal data as highlighted by the authors.[36] An alternative view, based on pathological studies describing tau pathology at a younger age than amyloid plaques,[7,37] is that hyperphosphorylation and amyloid plaque formation are independently occurring pathophysiological processes that share a common etiology.[38] Our findings of near-simultaneous change in amyloid and tau in a large database of intra-individual longitudinal CSF measurements support the view that tau phosphorylation accelerates at the very least soon after amyloid deposition has begun. That relatively modest amounts of amyloid deposition can have deleterious effects is supported by evidence that subthreshold amyloid accumulation in the negative amyloid range associates with worsening episodic memory ability.[5] Even prior to cognitive change, hypometabolism and atrophy have been shown to significantly accelerate more than 20 and 17 years, respectively, before participants reach amyloid positivity,[3] thus arguing against the requirement for widespread amyloid to trigger the pathophysiological cascade.

4.1 | Limitations

Although the amyloid latent class result performed well, the confidence in the p-Tau accumulators latent class model is lower. This highlights the well-recognized challenges to predicting who will develop tau pathology. Given that the best predictive power for future impairment comes from combining amyloid and tau measures in a ratio,[29,35,39] it may be that combined amyloid/p-tau progression models will be required to identify those at risk of converting clinically. The non-linear analysis should also be treated with caution given that individuals have an average of less than three measurements per person.

A further limitation is that we have used the term "accumulator" to account for both those who increase in the strength of their PET signal as well as progressively reduce their AD biomarker concentration levels in their CSF. This is likely an oversimplification as of the two only PET gives direct evidence of signal accumulation. In contrast, CSF metabolite levels are the result of a much more dynamic system, the balance between production and clearance[40] as well as preanalytical factors that have been shown to introduce variability.[41] Therefore, the term "accumulator" should be used with caution when CSF biomarker progression is concerned.

5 | CONCLUSIONS

The current analysis demonstrates the existence of distinct classes of amyloid and p-Tau accumulators. Given the accumulating evidence for pathological effects of subthreshold amyloid, this result underscores the importance of identifying individuals who are on the path to amyloid positivity and/or rapid tau phosphorylation. The currently available predictive models of these subclasses are modest, which emphasizes the need for further work on developing biomarkers that are phase-specific, that is, more relevant to the preclinical stage of the disease.

ACKNOWLEDGMENTS/CONFLICTS/FUNDING SOURCES

The BLSA study is supported by the Intramural Research Program of the National Institute on Aging. The BIOCARD study is supported in part by grants from the National Institutes of Health: U19-AG03365, and P50-AG005146. Ivan Koychev's work on the project was supported by the Medical Research Council – National Institute of Health Partnership in Neurodegeneration Award and Dementias Platform UK. Dr Mogekhar reports a research grant from Fujirebio Diagnostics Ltd that produces CSF biomarker assays, which however were not used in this particular study/analysis. Dr Albert is a consultant for Eli Lilly. The other co-authors report no other disclosures.

REFERENCES

1. Pillai JA, Cummings JL. Clinical trials in predementia stages of Alzheimer disease. *Med Clin North Am*. 2013;97(3):439-457.
2. Sperling RA, Rentz DM, Johnson KA, et al. The A4 study: stopping AD before symptoms begin? *Sci Transl Med*. 2014;6(228):228fs13.
3. Insel PS, Ossenkoppele R, Gessert D, et al. Time to amyloid positivity and preclinical changes in brain metabolism, atrophy, and cognition: evidence for emerging amyloid pathology in Alzheimer's disease. *Front Neurosci*. 2017;11:281.
4. Mattsson N, Insel PS, Nosheny R, et al. Emerging beta-amyloid pathology and accelerated cortical atrophy. *JAMA Neurol*. 2014;71(6):725-734.
5. Landau SM, Horng A, Jagust WJ, Neuroimaging AsD. Memory decline accompanies subthreshold amyloid accumulation. *Neurology*. 2018;90(17):E1452-E1460.
6. Leal SL, Lockhart SN, Maass A, Bell RK, Jagust WJ. Subthreshold amyloid predicts tau deposition in aging. *J Neurosci*. 2018;38(19):4482-4489.
7. Braak H, Del Tredici K. The pathological process underlying Alzheimer's disease in individuals under thirty. *Acta Neuropathol*. 2011;121(2):171-181.
8. Jack CR Jr., Knopman DS, Chetelat G, et al. Suspected non-Alzheimer disease pathophysiology—concept and controversy. *Nat Rev Neurol*. 2016;12(2):117-124.
9. de Leon MJ, Pirraglia E, Osorio RS, et al. The nonlinear relationship between cerebrospinal fluid Abeta42 and tau in preclinical Alzheimer's disease. *PLoS One*. 2018;13(2):e0191240.
10. Insel PS, Mattsson N, Donohue MC, et al. The transitional association between beta-amyloid pathology and regional brain atrophy. *Alzheimers Dement*. 2015;11(10):1171-1179.
11. Resnick SM, Goldszal AF, Davatzikos C, et al. One-year age changes in MRI brain volumes in older adults. *Cereb Cortex*. 2000;10(5):464-472.
12. Hixson JE, Vernier DT. Restriction isotyping of human apolipoprotein E by gene amplification and cleavage with HhaI. *J Lipid Res*. 1990;31(3):545-548.
13. Holland PM, Abramson RD, Watson R, Gelfand DH. Detection of specific polymerase chain reaction product by utilizing the 5'—-3' exonuclease activity of Thermus aquaticus DNA polymerase. *Proc Natl Acad Sci U S A*. 1991;88(16):7276-7280.
14. Soldan A, Pettigrew C, Li S, et al. Relationship of cognitive reserve and cerebrospinal fluid biomarkers to the emergence of clinical symptoms in preclinical Alzheimer's disease. *Neurobiol Aging*. 2013;34(12):2827-2834.
15. Miller MI, Younes L, Ratnanather JT, et al. The diffeomorphometry of temporal lobe structures in preclinical Alzheimer's disease. *Neuroimage Clin*. 2013;3:352-360.
16. Doshi J, Erus G, Ou Y, et al. MUSE: MUlti-atlas region Segmentation utilizing Ensembles of registration algorithms and parameters, and locally optimal atlas selection. *Neuroimage*. 2016;127:186-195.
17. Erus G, Doshi J, An Y, Verganelakis D, Resnick SM, Davatzikos C. Longitudinally and inter-site consistent multi-atlas based parcellation of brain anatomy using harmonized atlases. *Neuroimage*. 2018;166:71-78.
18. Jack CR Jr., Twomey CK, Zinsmeister AR, Sharbrough FW, Petersen RC, Cascino GD. Anterior temporal lobes and hippocampal formations: normative volumetric measurements from MR images in young adults. *Radiology*. 1989;172(2):549-554.
19. Ashburner J, Friston K. Multimodal image coregistration and partitioning—a unified framework. *Neuroimage*. 1997;6(3):209-217.
20. Jenkinson M, Bannister P, Brady M, Smith S. Improved optimization for the robust and accurate linear registration and motion correction of brain images. *Neuroimage*. 2002;17(2):825-841.
21. Jenkinson M, Beckmann CF, Behrens TE, Woolrich MW, Smith SM. Fsl. *Neuroimage*. 2012;62(2):782-790.
22. Zhou Y, Resnick SM, Ye W, et al. Using a reference tissue model with spatial constraint to quantify [11C]Pittsburgh compound B PET for early diagnosis of Alzheimer's disease. *Neuroimage*. 2007;36(2):298-312.
23. Proust-Lima C, Philipps V, Liquet B. Estimation of extended mixed models using latent classes and latent processes: the R Package lcmm. *J Stat Softw*. 2017;78(2):1-56.
24. Wood SN. Fast stable direct fitting and smoothness selection for generalized additive models. *J R Stat Soc B*. 2008;70:495-518.
25. Simpson GL. Modelling palaeoecological time series using generalized additive models. *bioRxiv*. 2018(322248).
26. Zhou P-b. Finite Difference Method. Numerical Analysis of Electromagnetic Fields. Berlin, Heidelberg: Springer; 1993: 63-94.
27. Sojkova J, Zhou Y, An Y, et al. Longitudinal patterns of beta-amyloid deposition in nondemented older adults. *Arch Neurol*. 2011;68(5):644-649.
28. Mattsson N, Insel P, Nosheny R, et al. CSF protein biomarkers predicting longitudinal reduction of CSF beta-amyloid42 in cognitively healthy elders. *Transl Psychiatry*. 2013;3:e293.
29. Mattsson N, Insel PS, Donohue M, et al. Predicting Reduction of Cerebrospinal Fluid beta-Amyloid 42 in Cognitively Healthy Controls. *JAMA Neurol*. 2015;72(5):554-560.
30. Bilgel M, An Y, Zhou Y, et al. Individual estimates of age at detectable amyloid onset for risk factor assessment. *Alzheimers Dement*. 2016;12(4):373-379.
31. Jansen WJ, Ossenkoppele R, Knol DL, et al. Prevalence of cerebral amyloid pathology in persons without dementia: a meta-analysis. *JAMA*. 2015;313(19):1924-1938.
32. Roe CM, Ances BM, Head D, et al. Incident cognitive impairment: longitudinal changes in molecular, structural and cognitive biomarkers. *Brain*. 2018;141(11):3233-3248.
33. Farrell ME, Chen X, Rundle MM, Chan MY, Wig GS, Park DC. Regional amyloid accumulation and cognitive decline in initially amyloid-negative adults. *Neurology*. 2018;91(19):e1809-e1821.
34. Landau SM, Horng A, Jagust WJ, Alzheimer's Disease Neuroimaging I. Memory decline accompanies subthreshold amyloid accumulation. *Neurology*. 2018;90(17):e1452-e1460.

35. Roe CM, Fagan AM, Grant EA, et al. Amyloid imaging and CSF biomarkers in predicting cognitive impairment up to 7.5 years later. *Neurology*. 2013;80(19):1784-1791.
36. Jack CR Jr., Knopman DS, Jagust WJ, et al. Tracking pathophysiological processes in Alzheimer's disease: an updated hypothetical model of dynamic biomarkers. *Lancet Neurol*. 2013;12(2):207-216.
37. Braak H, Braak E. Frequency of stages of Alzheimer-related lesions in different age categories. *Neurobiol Aging*. 1997;18(4):351-357.
38. Small SA, Duff K. Linking Abeta and tau in late-onset Alzheimer's disease: a dual pathway hypothesis. *Neuron*. 2008;60(4):534-542.
39. Fagan AM, Roe CM, Xiong C, Mintun MA, Morris JC, Holtzman DM. Cerebrospinal fluid tau/beta-amyloid(42) ratio as a prediction of cognitive decline in nondemented older adults. *Arch Neurol*. 2007;64(3):343-349.
40. Patterson BW, Elbert DL, Mawuenyega KG, et al. Age and amyloid effects on human central nervous system amyloid-beta kinetics. *Ann Neurol*. 2015;78(3):439-453.
41. Hansson O, Mikulskis A, Fagan AM, et al. The impact of preanalytical variables on measuring cerebrospinal fluid biomarkers for Alzheimer's disease diagnosis: A review. *Alzheimers Dement*. 2018;14(10):1313-1333.

SUPPORTING INFORMATION

Additional supporting information may be found online in the Supporting Information section at the end of the article.

How to cite this article: Koychev I, Vaci N, Bilgel M, et al. Prediction of rapid amyloid and phosphorylated-Tau accumulation in cognitively healthy individuals. *Alzheimer's Dement*. 2020;12:e12019.
https://doi.org/10.1002/dad2.12019